Applied Catalysis B: Environmental 84 (2008) 58–64

Contents lists available at ScienceDirect

Applied Catalysis B: Environmental

journal homepage: www.elsevier.com/locate/apcatb

# An EPR study of physi- and chemisorption of NO on MgO: Effect of outgassing temperature and nature of surface sites

Shinya Higashimoto [a,1], Guylène Costentin [a,*], Bernard Morin [a], Michel Che [a,b]

[a] Laboratoire de Réactivité de Surface, Université Pierre et Marie Curie-Paris 6, UMR 7609-CNRS, 4, Place Jussieu, 75252 Paris Cedex 05, France
[b] Institut Universitaire de France, France

ARTICLE INFO

*Article history:*
Received 10 October 2007
Received in revised form 22 February 2008
Accepted 3 March 2008
Available online 18 March 2008

*Keywords:*
MgO
Surface
Low coordination
NO
Probe
Physisorption
Chemisorption
EPR
FT-IR
Acidic sites
Basic sites
Outgassing temperature

ABSTRACT

The interaction of NO molecules with the surface of MgO has been studied by EPR as a function of outgassing temperature. Two different types of paramagnetic species are identified by EPR: physisorbed NO and chemisorbed $NO_2^{2-}$. They are formed upon specific adsorption of NO on Lewis acidic $Mg^{2+}$ and basic $O^{2-}$ sites, respectively. The concentration of NO and $NO_2^{2-}$ radicals depends on the outgassing temperature of MgO reaching a maximum at 1073 K. FT-IR measurements suggest that sites liberated upon thermal outgassing by removal of OH and carbonate groups adsorbed on MgO play a significant role in the increase of the concentrations of NO and $NO_2^{2-}$ radicals. The latter are possibly formed on low coordinated oxide ions close to cationic vacancies or $O_{4C}^{2-}$ of monoatomic step and $O_{3C}^{2-}$ from kinks and divacancies.



## 1. Introduction

Because nitrogen oxides are very toxic air pollutants mainly emitted from car emission exhausts, much work has been carried out on their elimination from the atmosphere in view of the vital importance of environmental protection [1–4]. Recently, one of the most effective $NO_x$ trap ($BaO/Al_2O_3$) for de$NO_x$ was discovered by Shinjoh et al. [5]. For this reason, the study of the interaction of NO with the surface of alkaline-earth oxides is very important for understanding and developing novel $NO_x$ storage catalysts.

MgO exhibits a simple rock salt structure and different types of site are known to exist on the surface, which are related to the surface cations ($Mg^{2+}$) and anions ($O^{2-}$) in low coordination (LC), i.e.; in five- (5C), four- (4C) and three-fold (3C) coordinations. It is generally accepted that the lower the coordination of $Mg^{2+}$ or $O^{2-}$ ions, the higher their reactivity, a conclusion based on reactivity measurements carried out with spectroscopies such as UV–vis [6–8], FT-IR [9–13], photoluminescence [14–19], and EPR [20–22], sometimes combined with quantum chemical calculations [23–27].

EPR can bring useful information on the interactions of adsorbed NO with the surface [28–30]. Lunsford observed two types of paramagnetic species upon adsorption of NO on fully dehydrated MgO, identified: (1) at 93 K as NO radicals perturbed by the surface electric field and (2) at room temperature (RT) as stable $NO_2^{2-}$ radicals [31].

More recently Di Valentin et al. [32] showed that NO is very weakly adsorbed on MgO terraces outgassed at 1173 K and forms dimers, $(NO)_2$, as confirmed by FT-IR. They also indicated that NO is adsorbed on $Mg_{LC}^{2+}$ and $O_{LC}^{2-}$ ions in low coordination on dehydrated MgO as physisorbed NO and chemisorbed $NO_2^{2-}$ radicals, respectively, on the basis of EPR results and quantum chemical calculations. Moreover, Zhang et al. [33] observed that the doping of MgO by $Na^+$, $Al^{3+}$ or $Zr^{4+}$ increased the concentration of chemisorbed species compared to pure MgO. This increase was interpreted in terms of local reconstruction phenomena leading to high indices faces and thus to $Mg_{LC}^{2+}$–$O_{LC}^{2-}$ pairs.

* Corresponding author. Tel.: +33 1 44 27 60 05; fax: +33 1 44 27 60 33.
*E-mail address:* costenti@ccr.jussieu.fr (G. Costentin).
[1] Present address: Department of Applied Chemistry, College of Engineering, Osaka Institute of Technology, Asahi-ku, Osaka 535-8585, Japan.

0926-3373/$ – see front matter © 2008 Published by Elsevier B.V.
doi:10.1016/j.apcatb.2008.03.004

Much attention has already been paid to the role of dehydroxylation of MgO in the formation of surface defects as followed by FT-IR [34–38], photoluminescence [19,39] and TPD-MS [40]. However, there is a lack of EPR data on the adsorption of NO on MgO as a function of the outgassing temperature. The aim of this paper is to follow quantitatively and qualitatively the formation of physisorbed NO and chemisorbed $NO_2^{2-}$ paramagnetic species on MgO surface as a function of outgassing temperature in order to identify the nature of the surface sites implied in their formation.

## 2. Experimental

MgO with large specific surface area was obtained from the decomposition of $Mg(OH)_2$. The latter was produced by hydrolysis of low surface area MgO (Aldrich, 99.99%) in hot water (353 K) for 12 h and further drying at 353 K for 6 h under dynamic primary vacuum ($10^{-1}$–$10^{-2}$ Torr, 1 Torr = 133.32 Pa). The sample was pretreated under secondary dynamic vacuum for 1 h ($10^{-5}$ Torr) to the nominal temperature in the range 300–1423 K at a rate of 1 K/min. The abbreviation, MgO-*T*, used thereafter corresponds to MgO outgassed at temperature *T* (K).

The specific surface areas were measured by $N_2$ adsorption on an automatic porosimeter (Micromeritics ASAP 2010) and calculated by the BET method. The relative error on the given BET values is estimated to be 5%.

Thermally outgassed MgO exhibited very weak hyperfine patterns due to $Mn^{2+}$ traces. EPR spectra of MgO in absence of NO were subtracted from those in presence of NO. After evacuation of MgO under the desired conditions, NO (20 Torr) was admitted onto the sample at room temperature in the quartz EPR tube.

The X-band EPR spectra were recorded at 77 K and room temperature on a Bruker ESP 300E equipped with a rectangular cavity. Concentrations of radicals were determined by double-integration and comparison with the number of spins of a reference solution of $CuSO_4{\cdot}5H_2O$ in water. For all experiments, the same cell was used with similar height of samples. In these conditions, the error on concentration measurements is of 10%.

For FT-IR measurements, semitransparent wafers of MgO of about 10 mg were obtained at a pressure of about $10^5$ Pa. MgO wafers were thermally outgassed following the same procedure as that used for EPR measurements. The IR transmission spectra were recorded using a Fourier transform IR spectrometer model IFS 66V (Bruker) with a resolution of 1 $cm^{-1}$.

## 3. Results

### 3.1. Effect of outgassing temperature of MgO on NO adsorption

After NO is adsorbed at RT on MgO-773, no EPR signal is observed at RT. However, at low temperature (77 K), an intense signal is observed (Fig. 1a): it is assigned to physisorbed NO with a hyperfine triplet ($I = 1$ for $^{14}N$) with a coupling constant (31 G ± 0.5) centered at $g_\perp = 1.995 \pm 0.005$. The other *g*-tensor component is found at $g_\parallel^\alpha = 1.875 \pm 0.002$.

On MgO-1073, a different signal (Fig. 1b) is observed at 77 K centered at $g_\perp = 1.995 \pm 0.02$ together with three independent $g_\parallel$ components
($g_\parallel^\beta = 1.888 \pm 0.001$, $g_\parallel^\gamma = 1.920 \pm 0.001$, $g_\parallel^\delta = 1.959 \pm 0.001$),
which are very consistent with the experimental and calculated data reported by Di Valentin et al. [32]. By computer simulation, the contribution of β, γ and δ species is estimated to be 65, 25 and 10%, respectively, on MgO-1073. From these data, it is found that the distribution of the different physisorbed NO radicals depends on the outgassing temperature of MgO.

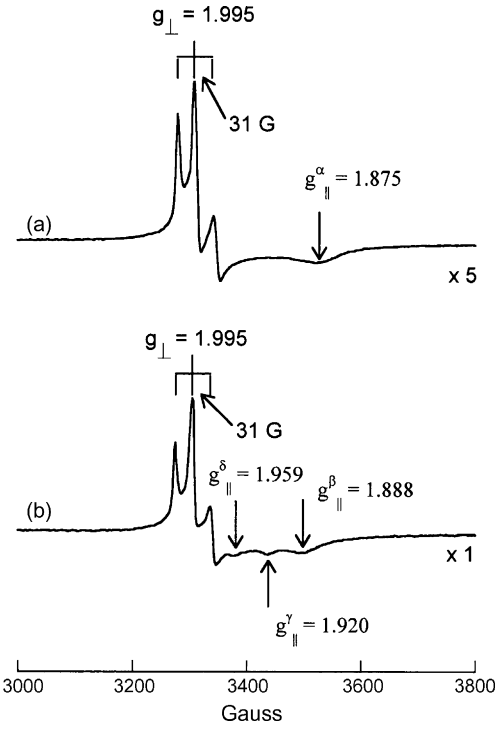


**Fig. 1.** EPR spectra (X-band, 77 K) of physisorbed NO species on MgO-773 (a) and on MgO-1073 (b).

By contrast, NO adsorbed on MgO-1073 exhibits at RT a weak signal (Fig. 2) strikingly different from the signals of Fig. 1. Table 1 gathers the magnetic parameters reported in the literature [32,41–43] for various nitrogen-containing radicals adsorbed on MgO and CaO. By comparison with data of Table 1, this signal is due to rather strongly bound and stable chemisorbed $NO_2^{2-}$ radical ions on the basis of its *g* values ($g_\perp = 2.007$ and $g_\parallel = 2.003$) and of the rather large nitrogen hyperfine coupling constant (40 G) [32].

The variations of concentration of paramagnetic NO and specific surface area are shown in Fig. 3 as a function of the outgassing temperature of MgO. Three temperature regions can be distinguished: (I) 473–973, (II) 973–1073 and (III) 1073–1423 K according to the magnitude of the concentration of physisorbed NO radicals. MgO outgassed below 473 K does not exhibit any EPR signal neither at 77 K nor at RT. Physisorbed NO species start to be observed at relatively low outgassing temperature (573 K) and

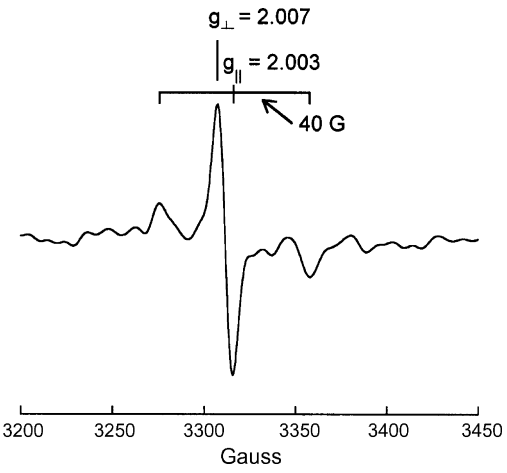


**Fig. 2.** EPR spectra (X-band, RT) of the chemisorbed $NO_2^{2-}$ species on MgO-1073.

**Table 1**
*g*-tensor and hyperfine tensor components of N-containing radicals adsorbed on various oxides

| System | Radical nature | $g_x$ | $g_y$ | $g_z$ | $A_x$ | $A_y$ (Gauss) | $A_z$ | Ref. |
|---|---|---|---|---|---|---|---|---|
| NO on MgO | $11e^-$ diatomic | 1.995 | 1.995 | 1.875 (α) | 31 | 0 | 0 | This work |
| | | 1.995 | 1.995 | 1.888 (α) | 31 | 0 | 0 | This work |
| | | 1.955 | 1.995 | 1.920 (β) | 31 | 0 | 0 | This work |
| | | 1.995 | 1.995 | 1.959 (γ) | 31 | 0 | 0 | This work |
| NO on MgO | 11e diatomic | 1.9948 | 1.998 | 1.8900 | 32 | 2.57 | 8.86 | [32] |
| | | 1.995 | 1.997 | 1.9188 | 32.5 | 0 | 0 | [32] |
| | | 1.995 | 1.996 | 1.9610 | 32.6 | 0 | 0 | [32] |
| $NO_2$ on MgO | $12e^-$ triatomic | 1.9915 | 2.002 | 2.005 | 49 | 67.4 | 53 | [41] |
| $NO_2^{2-}$ on MgO | $19e^-$ triatomic | 2.0100 | 2.0078 | 2.0044 | 40.6 | 0 | 0 | [32] |
| $NO_2^{2-}$ on MgO | $19e^-$ triatomic | 2.007 | 2.007 | 2.003 | 40 | 0 | 0 | This work |
| $NO_2^{2-}$ on CaO | $19e^-$ triatomic | 2.0033 | 2.0093 | 2.0069 | 33 | 0 | 0 | [42] |
| | | 2.0029 | 2.0091 | 2.0066 | 38 | 0 | 0 | [42] |
| | | 2.0023 | 2.0080 | 2.0075 | 33 | 0.5 | 0.5 | [42] |
| | | 2.0044 | 2.0080 | 2.0064 | 17.5 | 0.5 | 0.5 | [42] |
| $NO_2^{2-}$ on $TiO_2$ | $19e^-$ triatomic | 2.0060 | 2.0060 | 2.0040 | 0 | 0 | 31.3 | [43] |
| $NO_3$ on MgO | $23e^-$ tetraatomic | 2.003 | 2.009 | 2.014 | 0 | 0 | 0 | [41] |
| $NO_3^{2-}$ on CaO | $25e^-$ tetraatomic | 2.0044 | 2.0048 | 2.0048 | 37.3 | 41.8 | 41.8 | [42] |

their concentration progressively increases *versus* outgassing temperature, reaching a maximum at 1073 K. There is about a four-fold increase in region (II) with respect to region (I) followed by a drastic decrease at higher temperature (region III). The maximum concentration of paramagnetic NO radicals per $m^2$ for MgO-1073 is calculated to be approximately $8 \times 10^{16}$ spins/$m^2$.

Chemisorbed $NO_2^{2-}$ species start to be formed at 873 K, reach a maximum concentration at 1073 K and completely disappear at 1273 K. The specific surface area of MgO also varies as a function of the outgassing temperature, reaching a maximum after outgassing at 773 K.

There is obviously no simple correlation between the specific surface area and the concentration of NO radicals. These data suggest that the trend observed for NO species observed in regions (I) and (II) cannot be due to surface area changes only but rather to the formation of active sites on MgO available for specific interaction with NO. The decrease of both physisorbed NO and chemisorbed $NO_2^{2-}$ species in (III) are probably related to the sintering of MgO.

### 3.2. Effect of outgassing temperature on carbonates and hydroxyls removal

FT-IR measurements were performed to characterize the surface *versus* the outgassing temperature of MgO. The 1300–1500 $cm^{-1}$ region is associated with different stretching bands of carbonates on MgO [44]. As shown in Fig. 4a, the latter bands drastically decrease in intensity with increasing outgassing temperature and completely disappear for MgO-873.

Fig. 4b shows the FT-IR spectra in the 3600–3780 $cm^{-1}$ region related to O–H stretching vibrations. Two domains: (i) 3600–3650 $cm^{-1}$ and (ii) 3710–3780 $cm^{-1}$ are usually distinguished

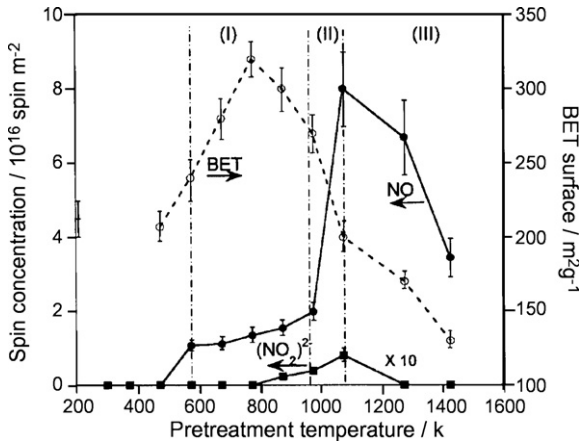


**Fig. 3.** Effect of outgassing temperature of MgO on the concentration of physisorbed NO (●), chemisorbed $NO_2^{2-}$ (■) radicals and BET surface (○).

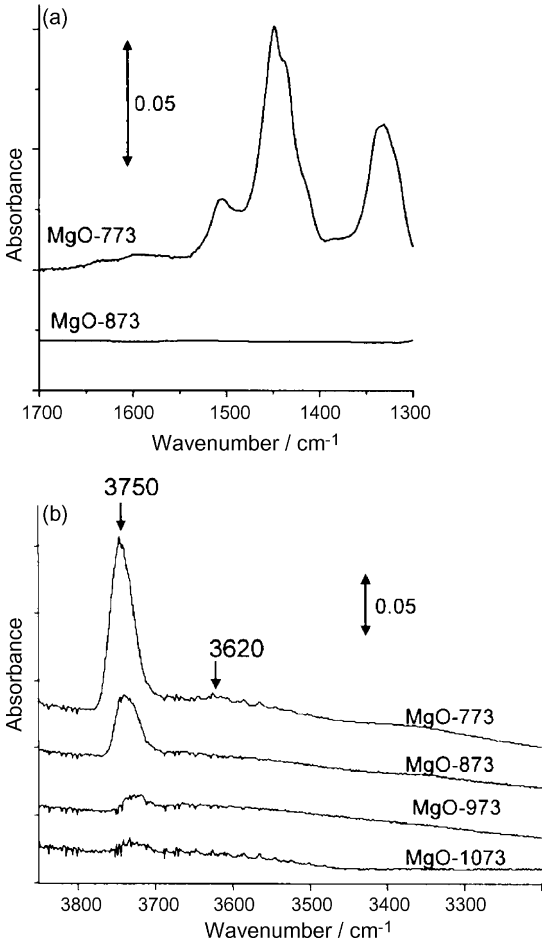


**Fig. 4.** FT-IR spectra recorded at RT for MgO-773 and MgO-1073 in the region of carbonate (a) and OH (b) stretching bands.

and their respective assignment is still a matter of debate [34–38]. The former domain was usually associated with O–H interacting via hydrogen bonds, whereas the narrow high frequency band was assigned to isolated groups [34–37]. However, new insights were recently proposed on the basis of the study of the hydroxylation of MgO surface sites involving low coordination ions: the calculation of thermal stability [27] and of the stretching frequency of different types of OH groups [38] enables to understand the evolution of experimental IR spectra with increasing outgassing temperature. It indicates that hydrogen bonding is the most important parameter, with also some dependence on the local topology of the surface. The broad low frequency band is assigned to hydrogen bond donor OH groups (issued from the protonation of surface oxide ion $O_{LC}^{2-}$) whereas hydrogen bond acceptor OH groups (formed on $Mg^{2+}$) and isolated groups (formed only on very specific surface irregularities such as kinks or divacancies [45]) are responsible for the narrow high frequency band.

From Fig. 4b, it is observed that the OH groups corresponding to the broad IR band at low frequency are first eliminated and disappear at 873 K, whereas those of the narrow high frequency band remain stable at higher temperature. It can be seen that the maximum of the narrow band is shifted to lower wavenumber upon temperature, which is consistent with its composite character [10,37,38]. Most OH groups are eliminated on MgO-1073. All these observations are consistent experimental data of literature [10,37] and with calculations of the thermal stability of the different types of OH groups [27] and indicate that the removal of hydroxyl groups of the high frequency band concerns OH groups formed on edges of steps, corners and finally isolated OH groups formed on kink and divacancies.

## 4. Discussion

The main result of this study concerns: (i) the effect of the outgassing temperature of MgO on the concentration of two different types of NO radicals, i.e., physi- NO and chemisorbed $NO_2^{2-}$ species and (ii) the nature of the surface sites.

### 4.1.1. Effect of outgassing temperature on MgO surface

It is well accepted that the dehydroxylation reaction: $Mg(OH)_2 \rightarrow MgO + H_2O$ takes place upon outgassing at around 573 K, first at the surface and then from the extended surface (terrace sites) into the bulk [46]. This phenomenon which leads to constraint and breaking of crystallites [47] is accompanied by an increase of surface area as shown in Fig. 3 in the temperature range below 773 K.

The sites liberated upon thermal outgassing lead to an increase of the concentration of physisorbed NO and chemisorbed $NO_2^{2-}$ radicals that are formed on $Mg^{2+}$ and $O^{2-}$ surface sites, respectively. Physisorbed NO species starting to be formed from 573 K, it implies that the $Mg^{2+}$ surface sites specific for their formation are liberated from this temperature. Because it is well established that MgO(1 0 0) terraces are dehydrated [48] and decarbonated [49,50] at room temperature, low coordinated $Mg_{4C,3C}^{2+}$ ions are most probably involved in the formation of physisorbed NO. In regions (I) and (II), the concentration of physisorbed NO radicals increases, which corresponds to the progressive disappearance of OH and or carbonates by departure of $H_2O$ and $CO_2$, respectively from these $Mg_{4C,3C}^{2+}$.

On the other hand, chemisorbed $NO_2^{2-}$ species start to be formed in region (II), i.e., above 873 K. Although $CO_2$ reacts with a large fraction of surface $O^{2-}$ sites to form carbonates, the total disappearance of the latter being reached at 873 K, they cannot directly influence the concentration of chemisorbed $NO_2^{2-}$ radicals. At reverse, the sites liberated from departure of OH groups formed by protonation of surface $O^{2-}$ sites are involved in the formation of chemisorbed $NO_2^{2-}$ species.

### 4.1.2. Physisorbed NO species on $Mg^{2+}$ sites

The interaction of NO with Lewis acidic $Mg^{2+}$ sites results in the crystal field splitting ($\Delta$) of the degenerate NO $p\pi^*$ antibonding orbitals into two levels, depending on the intensity of the crystal field as shown in Scheme 1. The relation between the splitting ($\Delta$) and $g_z$ is given by the following equation:

$$g_z = g_e - \frac{2\lambda}{\Delta}$$

where $z$ is chosen along the molecular axis of NO, $g_e = 2.0023$, $\lambda$ is the spin–orbit coupling constant of NO. The value of $\lambda$ is taken equal to 0.0015 eV for the NO molecule trapped on the surface of MgO [51]. From this equation, the $\Delta$ values are found to be (Table 2): ($\alpha$) 0.23 eV for MgO-773, and for the three different species in the sequence ($\beta$) 0.26 < ($\gamma$) 0.36 < ($\delta$) 0.69 eV for MgO-1073.

The $g_{\|}$ component ($g_z$) of the $g$-tensor was shown to sensitively depend on the charge of the adsorption site [29,52] and on the hydroxyl coverage [53]. This is shown by Table 2 which gives $g$-tensor components and $\Delta$ values of NO adsorbed on various oxides [31,53–59]: the larger the $\Delta$ splitting, the higher the charge and the degree of dehydration.

On the basis of present results, the surface active sites leading to species $\alpha$ (never reported earlier (Table 2)), appear to be more easily liberated than those which form species $\beta$, $\gamma$ and $\delta$. This implies that the $Mg^{2+}$ cations progressively liberated by the departure of hydrogen bond acceptor OH groups (edges of steps; corners) or isolated OH (formed on $Mg_{3C}^{2+}$ of kinks or divacancies) with high frequency IR vibration are involved in the formation of physisorbed NO species, $\alpha$ then $\beta$, $\gamma$ and $\delta$. Because it is expected that $Mg^{2+}$ cations of low coordination are liberated at increasing outgassing temperature, and that the lower the coordination state of the $Mg^{2+}$ cation, the stronger its acidity [27,60–63] it could be inferred that the stronger Lewis acidic $Mg^{2+}$ sites lead to higher $\Delta$ splitting. The different natures of physisorbed NO species are related to the interaction of NO

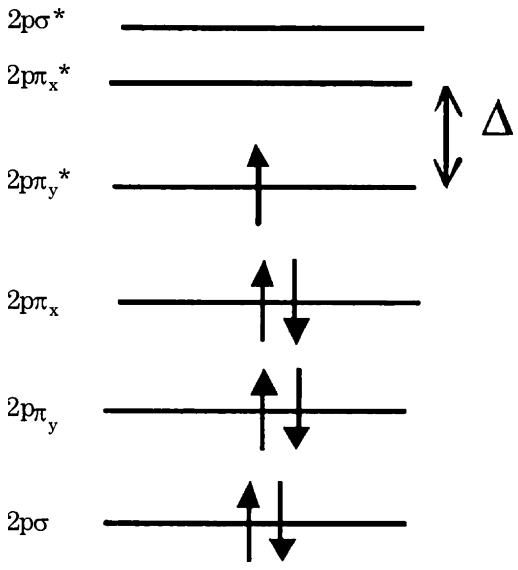


**Scheme 1.** Energy diagramme of the molecular orbitals of NO.

**Table 2**
*g*-tensor components and crystal field splitting $\Delta$ for NO adsorbed on various oxides

| System | Cation charge ($M^{n+}$) | $g_x$ | $g_y$ | $g_z$ | $\Delta$ (eV)[a] | Ref. |
|---|---|---|---|---|---|---|
| NO on NaY–zeolite | 1+ | 1.989 | 1.989 | 1.86 | 0.21 | [54] |
| NO on $Cu^+$/ZSM-5 | 1+ | 1.999 | 2.003 | 1.889 | 0.26 | [55] |
| NO on MgO | 2+ | 1.996 | 1.996 | 1.89 | 0.26 | [31] |
| NO on MgO | 2+ | 1.9948 | 1.998 | 1.8900 | 0.27 | [32] |
| | 2+ | 1.995 | 1.997 | 1.9188 | 0.36 | [32] |
| | 2+ | 1.995 | 1.996 | 1.9610 | 0.73 | [32] |
| NO on MgO-773 | 2+ | 1.995 | 1.995 | 1.875 ($\alpha$) | 0.23 | This work |
| NO on MgO-1073 | 2+ | 1.995 | 1.995 | 1.888 ($\beta$) | 0.26 | This work |
| | | 1.995 | 1.995 | 1.920 ($\gamma$) | 0.36 | This work |
| | | 1.995 | 1.995 | 1.959 ($\delta$) | 0.69 | This work |
| NO on ZnS | 2+ | 1.997 | 1.997 | 1.91 | 0.32 | [56] |
| NO on ZnO | 2+ | 1.999 | 1.999 | 1.94 | 0.48 | [56] |
| NO on silica–magnesia | 2+ | 1.996 | 1.996 | 1.95 | 0.57 | [53] |
| | 2+ | 1.996 | 1.996 | 1.91 | 0.32 | [53] |
| NO on $\gamma$-$Al_2O_3$ | 3+ | 1.996 | 1.996 | 1.96 | 0.71 | [53] |
| NO on silica alumina | 3+ | 1.997 | 1.997 | 1.95 | 0.57 | [53] |
| NO on silica alumina outgassed at 100 °C | 3+ | | | 1.87 | 0.23 | [53] |
| NO on AlHY zeolite | 3+ | | | 1.95 | 0.57 | [57] |
| NO on $TiO_2$ | 4+ | 2.003 | 2.003 | 1.920 | 0.36 | [58] |
| NO on $SnO_2$ | 4+ | 2.0002 | 2.0002 | 1.949 | 0.56 | [59] |

[a] $\Delta$ values calculated using the spin–orbit coupling constant $\lambda$ = 0.015 eV for NO [53].

molecules with different types of $Mg^{2+}$ sites, in relation with their coordination and acidic properties.

#### 4.1.3. $NO_2^{2-}$ species chemisorbed on $O_{LC}^{2-}$ sites

Quantum chemical calculations showed that NO adsorption on low coordinated $Mg_{LC}^{2+}$–$O_{LC}^{2-}$ pairs causes the localized bond formation between the $2p\Pi^*$ orbitals of NO and the lone pair of the lattice $O^{2-}$ anion [24]. The ability of $Mg_{LC}^{2+}$–$O_{L'C}^{2-}$ (L, L′ = 3, 4) pairs to stabilize NO as $NO_2^{2-}$ follows the order, $Mg_{3C}^{2+}$–$O_{3C}^{2-}$ > $Mg_{3C}^{2+}$–$O_{4C}^{2-}$ > $Mg_{4C}^{2+}$–$O_{3C}^{2-}$ > $Mg_{4C}^{2+}$–$O_{4C}^{2-}$ [24]. Indeed, in contrast to the cases of CaO [59] and BaO [64] where quite strong interaction with NO is expected, even on terraces, according to DFT calculations, no chemisorption of NO takes place on MgO(1 0 0) terraces [32]. Paganini et al. [42] reported that 0.5–1.0% of MgO surface fully dehydrated at 1123 K is covered upon NO adsorption by monomeric NO species. The present quantitative results show that, among NO species adsorbed on MgO-1073, 99% are physisorbed and only 1% are chemisorbed species. This indicates that less than 0.01% of surface sites participate in the formation of chemisorbed $NO_2^{2-}$.

Assuming perfect small cubes with an average size of ca. 180 Å as models of MgO particles, the relative amounts of $O_{5C}^{2-}$:$O_{4C}^{2-}$:$O_{3C}^{2-}$ ions are roughly estimated to be in the ratios $6 \times 10^3$:$1.3 \times 10^2$:1, respectively. In the real experimental system, the number of $O_{3C}^{2-}$ ions is higher than in the theoretical system because, beside corners, other types of $O^{2-}{}_{3C}$ ions can exist, such as kinks or divacancies [27], so that $O_{3C}^{2-}$ ions occupy more than 0.016% of the surface sites. It can thus be inferred that not all these basic low coordinated sites are involved in $NO_2^{2-}$ formation.

Consistently, Che et al. [65] studied by EPR one electron donor properties of MgO using tetracyanoethylene ($(CN)_2C=C(CN)_2$, TCNE) as probe molecule. The radical concentration of $TCNE^-$ on MgO preactivated at 973 and 1073 K, associated to coordinatively unsaturated $O^{2-}$ ions, was estimated to be three orders of magnitude larger than that of $NO_2^{2-}$ in the present study. This result implies that NO appears to be a more selective probe than TCNE. Because a thermally equilibrated crystal possesses a certain disorder in the form of Schottky defects which consist of isolated $Mg^{2+}$ or $O^{2-}$ vacancies [66], Lunsford suggested that magnesium cationic vacancies that increase the density of charge, and thus the basicity, of the surrounding $O^{2-}$ ions could be responsible for the formation of $NO_2^{2-}$ [28].

There is another possibility, if one considers the various types of low coordinated ions on MgO surfaces, as depicted on Fig. 5 [67]. Such irregularities on a Mg(1 0 0) surface were experimentally evidenced: from AFM studies on MgO surfaces [68–73], 4C ions are located on the edge of steps of various height and 3C ions correspond not only to corners of cubic particles but also to kinks or divacancies in monoatomic steps. From photoluminescence results, low coordinated $O_{4C}^{2-}$ and $O_{3C}^{2-}$ are liberated in a large temperature domain (from 600 to 1273 K), which is consistent with different local environments for these $O_{4C}^{2-}$ and $O_{3C}^{2-}$ ions. Moreover, $O_{3C}^{2-}$ ions are liberated at lower temperature than $O_{4C}^{2-}$ [74]. This unexpected result is however confirmed by DFT calculations [27] based on the formalism developed for alumina and titania surfaces [75–77]: the presence of concave area such as monoatomic steps (height of one Mg–O bond length) or kinks or divacancies confer a high thermal stability to the corresponding OH groups in relation to their ability to bridge with magnesium cations of the underlaying (1 0 0) plane [27]. As a consequence, OH

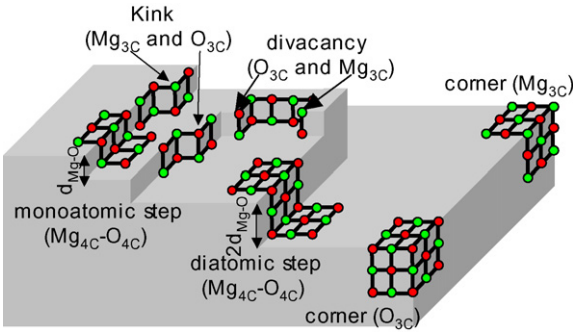


**Fig. 5.** Schematic representation of irregularities on the MgO surface. The steps and corners model, proposed by Che and Tench [67] is adapted to the systems discussed here. Defects modelled in the present work are shown with red ($O^{2-}$) and green ($Mg^{2+}$) spheres. (For interpretation of the references to color in this figure legend, the reader is referred to the web version of the article.)

formed on monoatomic steps are much more stable than those formed on higher steps and even more stable than those formed on corners. For the same reasons, OH formed on kinks or divacancies are more stable than those formed on $O_{3C}^{2-}$ corners [27]. Moreover, recent DFT calculations on infra red OH stretching frequencies [38] indicate that the related OH groups contributes to the most stable OH groups of the upper part of narrow infra red band. Thus, taking these results into consideration as well as the temperature range of formation of $NO_2^{2-}$ (773–1273 K) reported on Fig. 3, it can be inferred that the very specific $O_{4C}^{2-}$ ions of monoatomic step and $O_{3C}^{2-}$ ions from kinks and divacancies are the surface sites that participate in the formation of $NO_2^{2-}$.

## 5. Conclusion

NO molecules are able to probe the surface sites of MgO, i.e., acidic $Mg^{2+}$ and basic $O^{2-}$ sites leading to physisorbed NO and chemisorbed $NO_2^{2-}$ radicals, respectively. Their concentrations and the shape of their EPR spectra depend on the outgassing temperature of MgO. The following conclusions can be drawn:

(1) The surface sites liberated upon outgassing at increasing temperature by removal of OH and carbonate groups adsorbed on MgO play a significant role in the increase of NO concentration,
(2) Physisorbed NO species (α) are observed on partially dehydrated MgO,
(3) The different natures of physisorbed NO species (β, γ, δ) are related to the interaction of the NO molecules with different types of $Mg^{2+}$ sites, in relation with their acidic properties,
(4) Among paramagnetic radicals adsorbed on MgO-1073, 99% are physisorbed NO and only 1% are chemisorbed $NO_2^{2-}$ species,
(5) Chemisorbed $NO_2^{2-}$ species present in low concentration are formed upon very specific adsorption on basic sites, i.e., beside low coordinated oxide ions close to cationic vacancies, as proposed by Lunsford [28], $O_{4C}^{2-}$ sites on monoatomic steps and $O_{3C}^{2-}$ in divacancies or /and kinks can also be proposed. These results illustrate how the coordination chemistry of the anions [78], here devoted to solids and including surface topology, and conditions of thermal outgassing that result in exposure of the low coordinated $Mg_{LC}O_{L,C}$ pairs or, at reverse, to their covering by adsorbates (here, hydroxyl groups) is a key point to account for the reactivity of MgO surface toward the NO molecule.

## Acknowledgments

The authors gratefully acknowledge most helpful discussions with Prof. Elio Giamello (Turin University, Italy), Prof. Zbigniew Sojka (Jagiellonian University, Cracow, Poland) and Dr. Céline Chizallet (IFP, Solaize, France). They express their gratitude for the technical assistance of Jean-Marc Krafft for FT-IR measurements and also thank the ANR BASICAT (Project : ANR-05-JCJC-0256-01) for its financial support.

## References

[1] M. Iwamoto, H. Yahiro, Y. Mine, S. Kagawa, Chem. Lett. (1989) 213–216.
[2] M. Iwamoto, H. Hamada, Catal. Today 10 (1991) 57–71.
[3] M. Shelef, Chem. Rev. 95 (1995) 209–225.
[4] Photofunctional Zeolites, NOVA, 2000.
[5] H. Shinjoh, N. Takahashi, K. Yokota, M. Sugiura, Appl. Catal. B 15 (1998) 189–201.
[6] E. Garrone, A. Zecchina, F.S. Stone, Philos. Mag. B 42 (1980) 683–703.
[7] A. Zecchina, M.G. Lofthouse, F.S. Stone, J. Chem. Soc. Faraday Trans. I 71 (1975) 1476–1490.
[8] A. Zecchina, D. Scarano, Stud. Surf. Sci. Catal. 21 (1985) 71–81.
[9] S. Coluccia, F. Boccuzzi, G. Ghiotti, C. Morterra, J. Chem. Soc. Faraday Trans. I 78 (1982) 2111–2119.
[10] E. Knözinger, K.H. Jacob, P. Hofmann, J. Chem. Soc. Faraday Trans. 89 (1993) 1101–1107.
[11] E. Knözinger, O. Diwald, M. Sterrer, J. Mol. Catal. A 162 (2000) 83–95.
[12] S. Coluccia, A.J. Tench, R.L. Segall, J. Chem. Soc. Faraday Trans. I 75 (1979) 1769–1779.
[13] M.-L. Bailly, C. Chizallet, G. Costentin, J.-M. Krafft, H. Lauron-Pernot, M. Che, J. Catal. 235 (2005) 413–422.
[14] C. Chizallet, M.L. Bailly, G. Costentin, H. Lauron-Pernot, J.M. Krafft, P. Bazin, J. Saussey, M. Che, Catal. Today 116 (2006) 196–205.
[15] S. Coluccia, A. Barton, A.J. Tench, J. Chem. Soc. Faraday Trans. I 77 (1981) 2203–2207.
[16] V.A. Shvets, A.V. Kuznetsov, V.A. Fenin, V.B. Kazansky, J. Chem. Soc. Faraday Trans. I 81 (1985) 2913–2919.
[17] M. Anpo, Y. Yamada, Y. Kubokawa, S. Coluccia, A. Zecchina, M. Che, J. Chem. Soc. Faraday Trans. I 84 (1988) 751.
[18] M. Anpo, M. Che, Adv. Catal. 44 (1999) 119–257.
[19] M.-L. Bailly, G. Costentin, H. Lauron-Pernot, J.M. Krafft, M. Che, J. Phys. Chem. B 109 (2005) 2404–2413.
[20] E. Giamello, M.C. Paganini, D.M. Murphy, A.M. Ferrari, G. Pacchioni, J. Phys. Chem. B 101 (1997) 971–982.
[21] M.C. Paganini, M. Chiesa, E. Giamello, S. Coluccia, G. Martra, D.M. Murphy, G. Pacchioni, Surf. Sci. 421 (1999) 246–262.
[22] D.M. Murphy, R.D. Farley, I.J. Purnell, C.C. Rowlands, A. Yacob, M.C. Paganini, E. Giamello, J. Phys. Chem. B 103 (1999) 1944–1953.
[23] A.L. Shluger, J.D. Gale, C.R.A. Catlow, J. Phys. Chem. 96 (1992) 10389–10397.
[24] X. Lu, X. Xu, N. Wang, Q. Zhang, J. Phys. Chem. B 103 (1999) 5657–5664.
[25] A. D'Ercole, C. Pisani, J. Chem. Phys. 111 (1999) 9743–9753.
[26] D. Ricci, C. Di Valentin, G. Pacchioni, P.V. Sushko, A.L. Shluger, E. Giamello, J. Am. Chem. Soc. 125 (2003) 738–747.
[27] C. Chizallet, G. Costentin, M. Che, F. Delbecq, P. Sautet, J. Phys. Chem. B 110 (2006) 15878–15886.
[28] J.H. Lunsford, Adv. Catal. 22 (1972) 265–344.
[29] M. Che, E. Giamello, Stud. Surf. Sci. Catal. 57B (1990) 265–332.
[30] Z. Sojka, Catal. Rev. 37 (1995) 461–512.
[31] J.H. Lunsford, J. Chem. Phys. 46 (1967) 4347–4351.
[32] C. Di Valentin, G. Pacchioni, M. Chiesa, E. Giamello, A. Abbet, U. Heiz, J. Phys. Chem. B 106 (2002) 1637–1645.
[33] G. Zhang, T. Tanaka, T. Yamaguchi, H. Hattori, K. Tanabe, J. Phys. Chem. 94 (1990) 506–508.
[34] S. Coluccia, L. Marchese, S. Lavagnino, M. Anpo, Spectrochim. Acta 43A (1987) 1573–1576.
[35] P.J. Anderson, R.F. Horlock, J.F. Oliver, Trans. Faraday Soc. 61 (1965) 2754–2762.
[36] S. Coluccia, S. Lavagnino, L. Marchese, Mater. Chem. Phys. 18 (1988) 445–464.
[37] E. Knözinger, K. Jacob, S. Singh, P. Hofmann, Surf. Sci. 290 (1993) 388–402.
[38] C. Chizallet, G. Costentin, M. Che, F. Delbecq, P. Sautet, J. Am. Chem. Soc. 129 (2007) 6442–6452.
[39] W.W. Duley, J. Chem. Soc. Faraday Trans. I 80 (1984) 1173–1179.
[40] H. Dunski, W.K. Jozwiak, H. Sugier, J. Catal. 146 (1994) 166–172.
[41] J.H. Lunsford, J. Colloid Interf. Sci. 26 (1968) 355–360.
[42] M.C. Paganini, M. Chiesa, P. Martino, E. Giamello, J. Phys. Chem. B 106 (2002) 12531–12536.
[43] M. Che, C. Naccache, Chem. Phys. Lett. 8 (1971) 45–48.
[44] R. Philipp, K. Omata, A. Aoki, K. Fujimoto, J. Catal. 134 (1992) 422–433.
[45] C. Chizallet, G. Costentin, J.-M. Krafft, H. Lauron-Pernot, M. Che, Chem. Phys. Chem. 7 (2006) 904–911.
[46] T. Yoshida, T. Tanaka, H. Yoshida, T. Funabiki, S. Yoshida, T. Murata, J. Phys. Chem. 99 (1995) 10890–10896.
[47] J.F. Goodman, Proc. Roy. Soc. (Lond.) A 247 (1958) 346–352.
[48] M.J. Stirniman, C. Huang, R.S. Smith, S.A. Joyce, B.D. Kay, J. Chem. l Phys. 105 (1996) 1295–1298.
[49] G. Pacchioni, J.M. Ricart, F. Illas, J. Am. Chem. Soc. 116 (1994) 10152–10158.
[50] G. Pacchioni, Surf. Sci. 281 (1993) 207–219.
[51] M. Chiesa, E. Giamello, D. Murphy, G. Pacchioni, M.C. Paganini, R. Soave, Z. Sojka, J. Phys. Chem. B 105 (2001) 497–505.
[52] K. Dyrek, M. Che, Chem. Rev. 97 (1997) 305–331.
[53] J.H. Lunsford, J. Catal. 14 (1969) 379–385.
[54] J.H. Lunsford, J. Phys. Chem. 72 (1968) 4163–4168.
[55] Z. Sojka, M. Che, E. Giamello, J. Phys. Chem. B 101 (1997) 4831–4838.
[56] J.H. Lunsford, J. Phys. Chem. 72 (1968) 2141–2144.
[57] K.M. Wang, J.H. Lunsford, J. Catal. 24 (1972) 262–271.
[58] M. Primet, M. Che, C. Naccache, M.V. Mathieu, B. Imelik, J. Chim. Phys. 67 (1970) 1629–1635.
[59] C. Di Valentin, A.A. Figini, G. Pacchioni, Surf. Sci. 556 (2004) 145–158.
[60] G. Pacchioni, T. Minerva, P.S. Bagus, Surf. Sci. 275 (1992) 450–458.
[61] J. Sauer, P. Ugliengo, E. Garrone, V.R. Saunders, Chem. Rev. 94 (1994) 2095–2160.
[62] K.M. Neyman, N. Rösch, Surf. Sci. 297 (1993) 223–234.
[63] R. Soave, G. Pacchioni, Chem. Phys. Lett. 320 (2000) 345–351.
[64] M.M. Branda, C. Di Valentin, G. Pacchioni, J. Phys. Chem. B 108 (2004) 4752–4758.
[65] M. Che, C. Naccache, B. Imelik, J. Catal. 24 (1972) 328–335.
[66] C.G. Harkins, W.W. Shang, T.W. Leland Jr., J. Phys. Chem. 73 (1969) 130–141.

[67] M. Che, A.J. Tench, Adv. Catal. 31 (1982) 77–133, and AERE Report-R9971, November 1980, 1-55.
[68] P. Liu, T. Kendelewicz, G.E. Brown, G.A. Parks, Surf. Sci. 412–412 (1998) 287–314.
[69] P. Liu, T. Kendelewicz, G.E. Brown, Surf. Sci. 412–413 (1998) 315–332.
[70] T.V. Ashworth, C.L. Pang, P.L. Wincott, D.J. Vaughan, G. Thornton, Appl. Surf. Sci. 210 (2003) 2–5.
[71] C. Barth, C.R. Henry, Phys. Rev. Lett. 91 (2003), 196102/196101–196102/196104.
[72] S.A. Holt, C.F. Jones, G.S. Watson, A. Crossley, C. Johnston, C.J. Sofield, S. Myhra, Thin Solid Films 292 (1997) 96–102.
[73] D. Scarano, S. Bertarione, G. Spoto, A. Zecchina, Surf. Sci. 570 (2004) 155.
[74] C. Chizalle, G. Costentin, H. Lauron Pernot, J.M. Krafft, M. Che, F. Delbecq, P. Sautet, in preparation.
[75] M. Digne, P. Sautet, P. Raybaud, P. Euzen, H. Toulhoat, J. Catal. 226 (2004) 54–68.
[76] C. Arrouvel, M. Digne, M. Breysse, H. Toulhouat, P. Raybaud, J. Catal. 222 (2004) 152–166.
[77] M. Digne, P. Sautet, P. Raybaud, P. Euzen, H. Toulhoat, J. Catal. 211 (2002) 1–5.
[78] K. Bowman-James, Acc. Chem. Res. 38 (2005) 671–678.